Plant Archives Volume 20 No. 2, 2020 pp. 5505-5515 **e-ISSN:2581-6063 (online), ISSN:0972-5210**

SELECTIVE COLORIMETRIC MERCURY IONS SENSING IN DIFFERENT SAMPLES USING SILVER NANOPARTICLES PREPARED FROM GINGER EXTRACT

Maryam Abdulghafor Ahmed, Abdulkadir Mohammed NooriJassim* and Salam A.H. AL-Ameri

Chemistry Department, College of Science, Mustansiriyah University, Baghdad, Iraq.

Abstract

A Bionanotechnology process was used as an ecological and price valuable methods to produced Nano-particles and Nano-materials. This study verifies the capability of *Ginger (Zingiber officinale*) plant extract developed at *in vitro* conditions for the silver nanoparticles (AgNPs) biosynthesis. The Surface Plasmon Resonance established at 430 nm demonstrated the AgNPs formation. Furthermore, SEM, AFM results explain that the nanoparticles had a spherical morphology. Additionally, UV-Vis, FTIR, Zeta potential study were agreed out to classify the produced AgNPs is effectively used for the detection of ecologically dangerous mercury ions in aqueous media through colorimetric process. Additionally, it has been established that the AgNPs illustrate good response towards mercury ion. The suggested method can be effectively used for the estimation of Hg (II) ions in tap, real water and albumin samples at low levels.

Key words: *Ginger (Zingiber officinale*), Silver Nanoparticles, Antioxidant, Mercury detection, Colorimetry.

Introduction

Nanoparticles (NPs) are investigated in various fields which consist of healthcare, environment, chemical production, makeup, electronics, chemical manufacturing, water management, catalyst, mechanics, optics, sensors (Mousavi *et al.*, 2017). Presently, the request for NPs was assembly by combination during biological, physical and chemical techniques (Zhang *et al.*, 2017). Currently, Nanoscience is a quickly developing field provided to manufacture an extensive range of different metal NPs. Silver is the mainly good metal in production of NPs owing to its extensive range of bactericidal and fungicidal behaviors and ability to link with diverse ligands and macromolecules in microbial cell. Silver has been usually use in manage of microbial formation as well as medicinal injury owing to its anti-inflammatory effect (Hamouda, *et al.*, 2019).

Furthermore, these NPs in colloidal forms are extra appropriate for biological uses since the formula do not include any hazard chemicals. While, careful selection is essential in this situation to find out the plant whose extracts contain excellent reducing with stabilize influence (Samrot *et al.*, 2018 Samrot *et al*., 2018, Behravan *et al.*, 2019, Priyadarshini *et al*., 2012, Murugan *et al*., 2014). Moreover, studies shown that the flavonoids, polysaccharides, enzymes, terpenoids and more proteins. The types of components here in the plants extracts reduce the silver ions with stabilize the Nps (Megarajan *et al*., 2016). As a piece of the constant caution to observe plant extract contain potential value in synthesis of silver nanoparticles. (Kumar *et al*., 2017. Kumar *et al.*, 2016. Kumar *et al*., 2017. Kumar *et al*., 2017. Dinda *et al.*, 2017) *Ginger (Zingiber officinale*) Roscoe (family *Zingiberaceae*) is generally cultured for its medicine uses and as a condiment. It is usually used to care for the regular cold, headache also rheumatic disorder(Yang *et al.*, 2009).

Several studies contain examined the phytochemical formulation of its rhizomes, informative zingiberene, gingerol, shogaol with their derived as the main components (Sivasothy *et al*., 2011). Ginger pharmacological activities Information contain antimicrobial, antioxidants, anti-inflammatory, hepato-protective also antinociceptive (Mostafa andSingab, 2016). The applying of natural nanotechnology for the improvement of selective as well as sensitive estimation methods in the analytical and biological sciences has been essential (Huang *et al*., 2013. Yoosaf *et al*., 2007).

Author for correspondence : E-mail : kadirchem@yahoo.com

Mercury is marked as harmful contaminant; between many mercury forms, the mainly stable also water soluble is Hg (II) ions which causes a threat to human health and it's nearby during the food chain. (Bernhoft, 2012). Chiefly, colorimeteric procedures have a special advantage owing to the easily, quickly, good selectivity moreover simplicity of use as well as quantitative and qualitative determination (Li *et al.*, 2010. Karthigaand Anthony, 2013). In this study, a procedure and discuss of the biosynthesis of AgNP by Ginger extract as a substitute to poisonous chemical materials and its using for Hg(II) colorimetric estimation.

Materials and Methods

Materials

Ginger was taking from locally commercial markets in Baghdad, Iraq. Silver nitrate, Mercury chloride, the chemicals and salts of metals, reagents and substances are of analytical grade purity purchased from BDH, Sigma Aldrich and Merck. Distilled water was employed through this work.

Preparation of Ginger extract

The impurities were removed from ginger using distilled water. The Ginger was peelings and cut it into very small pieces then put it in the mixer some time until it turns into juice, then it filtered with a piece of gauze to get clear of the fibers and later filtered through filter No. 1 to get the extract which stored at 4°C until use.

Synthesis AgNPs using Ginger

Biosynthesis of AgNPs: take 7 mL of the AgNO3 solution (0.5mmol/L) and added 0.5 mL of Ginger extract in a round-bottom flask. Heated the mixture at 100°C and the color of reaction media was gradually turned to yellow which indicating the AgNPs formation (50 min was recorded) (Nan *et al*., 2017).

Characterization of AgNPs:

The AgNPs formation were proved by determining the λ_{max} of the reaction mixture in LABOMED UV 2960 UV-Vis double beam spectrophotometer equipped with PC and 1cm quartz cell at 300-800 nm (Surya *et al*., 2016). After the preparation of AgNPs, they were centrifuged for 15 minutes at 5000 rpm. The procedure was repeating 3-5 times. The precipitate was taken and dried at 40°C for 4 hrs. For similarity, the dried AgNPs and Ginger powder were analyzed via FTIR, Tests cane, Shimadzu model using KBr and CsI discs in the range of 500-4000 cm^{-1} (Al-Alwani *et al*., 2015). AFM was employed to study the size and division circulations of the NPs. The evaporation procedure of the dropper was use to prepare AFM samples of suspension fluid. The SEM was used to describe the type and morphology of biological AgNPs formed. Measurements of Zeta potential was used to distinguishing the nano-material. Size of NPs was measured by electrophoretic Light Scattering (ELS) as well as Dynamic Light Scattering (DLS) using Zeta Plus.

Antioxidant activity:

Qualitative Determination of Free Radical by (TLC):

The antioxidant ingredient was analyzed via thin layer chromatography (TLC) followed by DPPH. A100µg of a Ginger extract, AgNPs and Gallic acid as standard solution were placed on TLC plates. The active antioxidant Ginger, AgNPs and Gallic acid showed yellow spots versus a violet background(Cuendet *et al*., 1997).

Quantitative free radical Determination via DPPH method:

The *Ginger* extract scavenging activity using DPPH method was tested *in vitro* as illustrated with little change (Shimada *et al.,* 1992). Gallic acid was use as standard. The quantities of sample needed to reduce the first DPPH concentration by 50% signify to the IC_{50}.

Colorimetric detection of mercury ions:

Ginger extract was used in the biosynthesis of AgNPs for colorimetric estimation of Hg (II) metal ions in aqueous media, 1 ml of recently prepared AgNPs were transfer to a glass test tubes, also 1 ml of 60 ppm of Hg (II) with further metal ions Fe^{+3}, Mg^{+2}, Co^{+2}, Zn^{+2},Cr^{+3}, Cu^{+2}, Mn^{+2}, Ni^{+2}, Ca^{+2} and Sn^{+2} metal ions were adding. Consequently, the changes in the color and absorbance spectra were observed using a UV-Vis spectrophotometer behind developing and taken a picture of the solutions by a camera (Chowdhury *et al*., 2015. Firdaus *et al.*, 2017).

The minimum detectable concentrations of Hg (II) Heavy metal ions for sensor studies were established by titration various Hg ion concentration versus AgNPs. Sensor workings were accepted by preparation of 60 ppm $HgCl_2$ standard solutions through a successive dilution. Behind gentle mixing, 1 mL aliquots of Hg (II) solution at final concentrations of 1.5, 2.5, 5, 7.5, 10, 12.5, 15, 17.5, 20, 22.5, 25, 27.5, 30 ppm were added singly into each one test tube. After shaking, set aside for 15min at room temperature, the UV-Vis spectra, SPR maximum of AgNPs at 430 nm and photos of the solutions were taken (Xu *et al*., 2018). The limit of detection (L.O.D) for Hg (II) ions was calculated by formula: LOD=3Sd/s, where 'SD' is the blank solution Standard Deviation, while 's' is the calibration curve slope.

Preparation of real samples

A-Water Samples:

For real water samples, tap water from our site (Mustansiriyah University, College of Science and Department of Chemistry) and Dyalah river water samples were collected. Every sample collected were spike with a fitting volume of 20-60 ppm Hg (II) standard solution and carefully mixed, filtered via a 0.2 µm membrane then centrifuged at 9000 rpm for 20 min. All samples were prepared under the same conditions and examined by UV–VIS spectra along with the suggested method. To confirm reproducibility, all testing were repeating 3 times (Farhadia *et al.*, 2012).

B- Preparation of bovine serum samples:

A 0.1% concentration bovine serum stock solution was prepared in D.W. The suspension was shacked as well as centrifuging for 30 min and 9.0 mL of this solution was mixed with 1.0 mL of 100 µg/ml Hg (II) solution (Kim *et al.*, 2018).

To determine the efficiency of the suggested method, Hg (II) concentrations adding in tap, river water as well as serum of bovine were calculated through 1mL of the AgNPs solution following by UV-VIS spectra. The dilution effect of each sample was considered.

Results and Discussion

Synthesis and Characterization of AgNPs

The *Ginger* extract have several reducing phytocomponds. The recently prepared Ginger extract colors remain unchanged after incubated for five days with $AgNO_3$ solution. Unusually, at the same time as expose to heating up to 100ºC, the extract having $AgNO_3$ twist from light pale yellow to dark brownish yellow, indicating the AgNPs formation. In the absence of $AgNO_3$, the extract didn't show any color alteration even exposing to 1h of heating. The results indicate the important of the heating for AgNPs preparation. The maximum practical AgNPs absorbance was showed at 430nm, which characteristic the SPR for AgNPs, Fig. 1.

The FTIR spectra of *Ginger* extract with AgNPs were illustrated in Fig. 2. The reactive groups could be found at a broad band centered at 3393.14 Cm^{-1} is assign to stretching vibrations of -OH and -NH groups of phyto-constituent find in this current Ginger extract. The peak at 2928.38 cm^{-1} is assigning to stretching vibration of C-H. The C=O stretching and N-H bending bands are overlapping and show a wide peak among 1863.86-1516 cm^{-1} with a 1638 cm^{-1} as a center. Side chain vibrations found at 1375 cm^{-1} Peak. All vibration bands are capable and relations for the Ginger extract carbohydrates as well as portions. As proved from Fig. 2, the AgNPs FTIR spectra showed all the Ginger extract vibration bands, which proposed that the NPs be stabilized via the phyto-components. Prior studies show that the phyto-proteins have an affinity to create a photo-induced electron transfer for the metal ion reducing (Megarajan *et al.*, 2016). As a result proved that the biological components found in Ginger extract refereed the photo-induced AgNPs syntheses also stabilize the NPs in the aqueous solutions.

Atomic Force Microscope, AFM was employed to identify the surface morphology as well as topography. The AgNPs prepared by using Ginger plant extract were studied using AFM. AFM surface analysis requires good attention because of factors that affect results such as tip or pollutions. AFM gives a three dimensional image of the nanoparticles surface at an atomic level. The average particle diameters were calculated in nano-scale size (Kyeyune, 2017). AFM surface analysis of silver nanoparticles, AgNPs shows the three-dimensional image of AgNPs as well as the average diameter of 53.45 nm, Fig. 3.

The SEM study revealed that the AgNPs have a different shape and sizes which consist of spherical NPs range from 22-33 nm, Fig. 4.

The presence of Ag element in AgNPs formula was

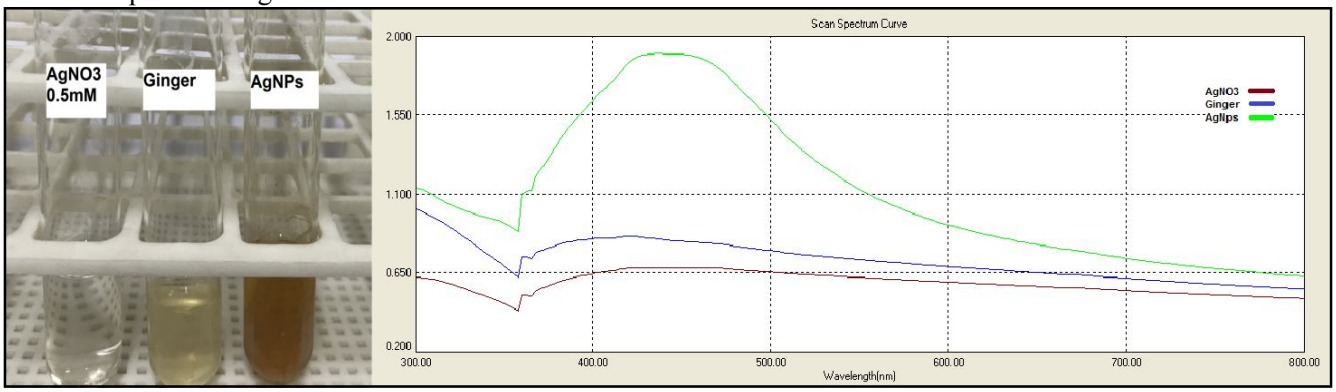

Fig. 1: UV-Vis spectra and Photo-image of color changing in $AgNO_3$, *Ginger* and synthesized AgNPs reaction mixture.

established via EDS microanalysis, Fig. 5. This spectrum shows a signal in the silver region. Metal silver Nano crystals display a typical absorbance peak near 3 keV owing to the SPR (Jagtap and Bapat, 2012. Awad *et al.*, 2014). Another signals for added C, N, O, Na, Mg, P, S, Cl, K and Ca metals here in the reaction solution confirmed to the extracellular Ginger extract organic components were found on the AgNPs surface or proximity.

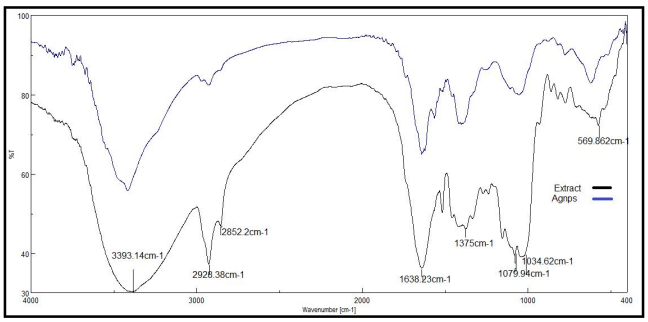

Fig. 2: The FTIR spectrums of *Ginger* extract and synthesized AgNPs.

The stability of the NPs was measures by Zeta potential (or in general, particles) in the colloidal suspension. The zeta potential value measured by (ELS) for Ginger extract was -17.88 mV with mobility value equal to -1.40 (μ/s)/(V/cm), whereas for the AgNPs was -22.5 mV and -2.11, respectively, Fig. 6. These suggest that the AgNPs electrical boundaries are relatively separate and decreased the NPs from more aggregating. The ELS is originally used for characterized the charges on the surface of colloidal particles or other macromolecules in an electric field for liquid media (Okubo and Suda, 1999). So, the obvious data indicated that the elements in liquid media are relatively unstable due to the zeta potential value was a lesser than ±30 mV and it was more stable as colloidal NPs than that was found in extract solution.

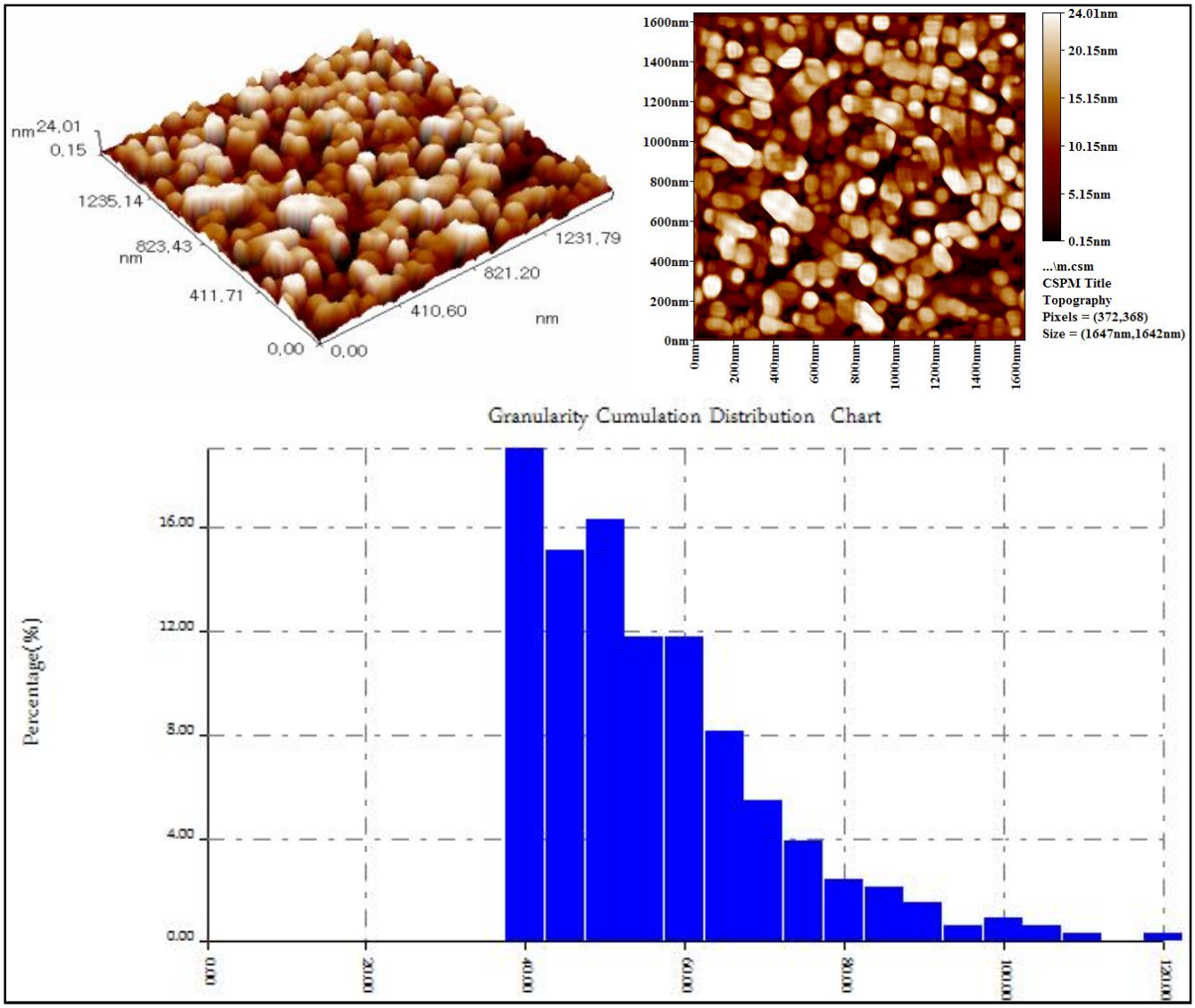

Fig. 3: AFM photo also size distributions of Ginger synthesis AgNPs.

Poly disparity is an amount for distribution of AgNPs from 0.000 to 0.5. When this value was higher than 0.5, this indicates an aggregation of NPs (Mostafa, 2018). The effective diameter and poly disparity for Ginger extract measured by DLS was equal to 636.90 nm, 0.225 while for synthesized AgNPs was equal to 211.85 nm, 0.215 respectively. Hence, this poly disparity value, 0.225 confirmed that the AgNPs synthesized by Ginger extract does not aggregate.

Antioxidant activity using TLC and DPPH methods:

The main antioxidant mechanism in foods is radical scavenging activity. So, a different method in which antioxidant activity has been measured by scavenging synthetic radical in organic solvents, mainly polar one such as methanol (Huang *et al.*, 2005). In scavenging activity method, DPPH is one of the hard and saleable important organic nitrogen radical, has UV-Vis absorbance at 517 nm (Rajakannu *et al*., 2015). Here in study, the antioxidant activities of Ginger extract was determined by free radical scavenging activity.

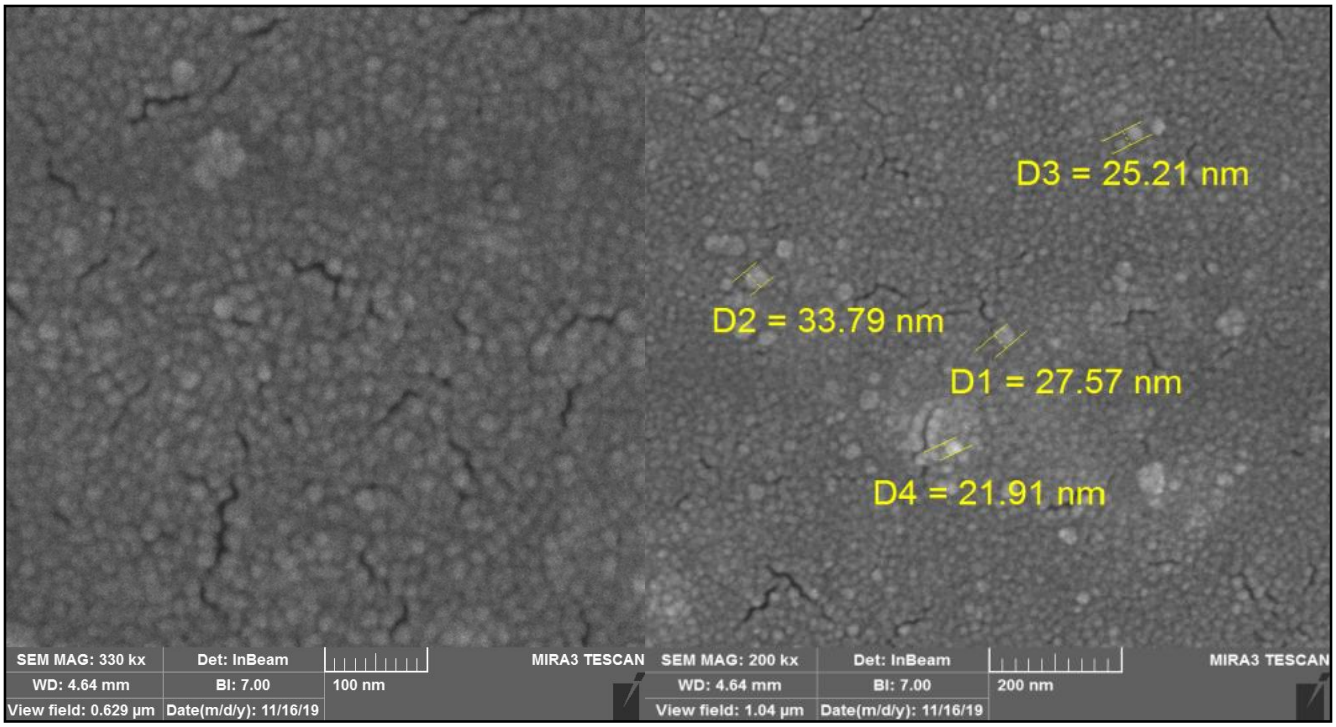

Fig. 4: SEM AgNPs images (Left=200 nm, Right=100 nm).

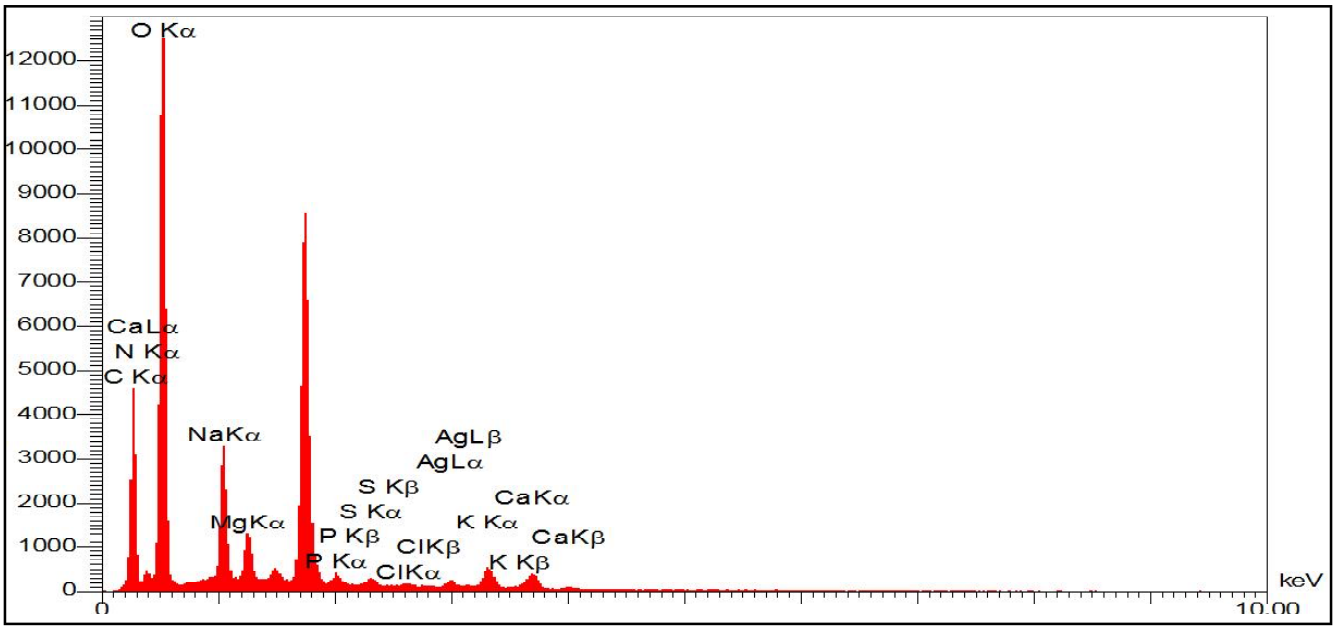

Fig. 5: EDS pattern of spherical AgNPs synthesized using Ginger.

The color variations from purple to yellow as the molar absorptivity of the DPPH radical at 517 nm decrease upon the move of acidic H-atom from the complex to DPPH radical to form DPPH-H. The resultant decolorization is stoichiometric with admiration to a total of electrons captured.

Radical scavenging properties of Gallic acid and Ginger extract were evaluated against the DPPH radical. The DPPH method shows that the extract has a potent scavenging activity as compare to standard Gallic acid.

Radical-scavenging possessions of a standard Gallic acid, *Ginger* extract and AgNPs were estimated in contradiction of the DPPH radical. The DPPH test was used to study the quantitative scavenging activity for three samples. Via using DPPH as a TLC spray, standard Gallic acid and *Ginger* extract seemed as clear yellow spots versus a purple background, Fig. 7. It means that they have a strong scavenging activity, while the AgNPs indicated less scavenging activity, table 1.

current consequences show the scavenging activity for extract and AgNPs associated with Gallic acid as a standard, It is observable from the data that radical scavenging activity of the interest compounds increased with the increasing of exhibiting concentration, its dose reliant on nature (Nurmahani *et al.*, 2012). The consequences show that it has a strong scavenging activity with IC50 standard Gallic acid of 31 µg/mL, while it were lower than IC_{50} value for every one of Ginger extract and created AgNPs.

Colorimetric detection of mercury ions (Metal sensors)

Toxic ions released from industrial liquid waste or natural sources, discharged into a river or the sea have serious effects to the environment as well as health. Mercury ion is one of these metals that may be present in usual source such as water, soil, air and synthetic pollutants, which causing significant health damage to the human body, if they are present in excess (Prasad *et al.*, 2018). Subsequently, the selective detection of mercury ions at very little concentration has a great interest in wastewater also biological methods (Clarkson *et al.*, 2003). Different procedures have been developed for Hg^{2+} estimation as sensor probes such as fluorescence (Yuan *et al.,* 2007), oligonucleotides (Wang *et al.*, 2010), polymers (Ayranci *et al.*, 2017), metallic nanoparticles (Kumar *et al.,* 2017) and semi-conducting quantum dots (Ke *et al.,* 2014). Metal nanoparticles (MNPs) methods based on colorimetric heavy metal ions detection illustrate a capable technique at low levels detection (Annadhasan and Rajendiran, 2015). Silver nanoparticles (AgNPs) have

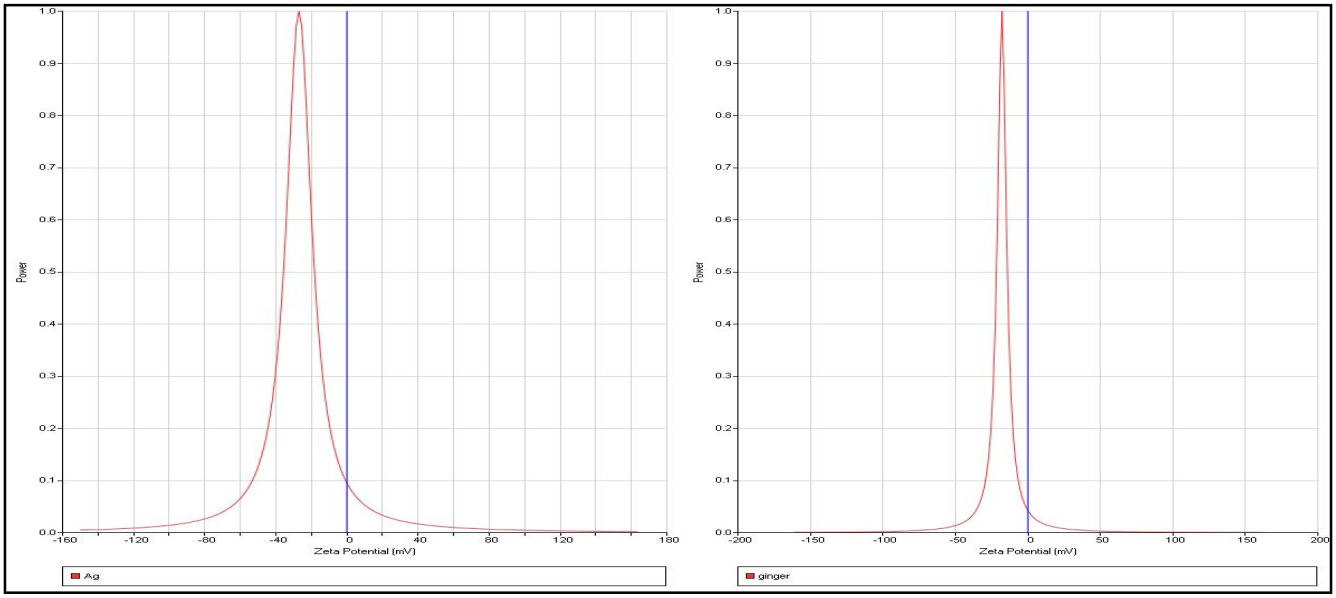

Fig. 6: Zeta potential distribution of Ginger(Left) and AgNPs (Right).

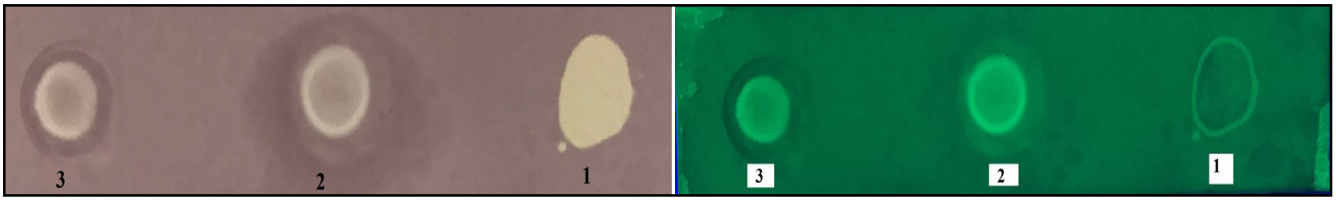

Fig. 7: The TLC photo-image (Left) and under UV-light (Right) for (1) Gallic Acid, (2) Ginger extract, (3) AgNPs.

Table 1: The DPPH model inhibition percent of *Ginger* extract and AgNPs at various concentrations (µg/mL).

Concentrations (µg/ml)	% Inhibition (standard solution-gallic acid)	% Inhibition (Ginger extract)	%Inhibition (AgNPs)
10	43.2	3.44	10.2
20	46.5	6.68	12.5
40	53.5	9.2	17.2
60	59.6	11.8	22.3
80	62.3	13.3	26.1
100	82.5	20.4	30.4

extra importance among different metallic nanoparticles for developing a mercury sensor, especially suitable to low cost and easy prepared (Kumar *et al.,* 2017), LSPR of AgNPs is extremely sensitive to little experiential changes in spectroscopic and visual methods (Chen *et al.,* 2016) broad of oxidation- reduction chemistry among Hg^{2+} and Ag° in AgNPs which forming Ag-Hg amalgam via nanoparticals etching (Atkins and de Paula, 2009) and examine the SPR AgNPs properties to detect Hg^{2+} ions. The adding of heavy metal salts at 60 ppm concentration of Mg^{2+}, Ca^{2+}, Cr^{3+}, Mn^{2+}, Fe^{3+}, Co^{3+}, Ni^{2+}, Cu^{2+}, Zn^{2+}, Hg^{2+} to AgNPs freshly prepare illustrate a yellow color excepting Hg^{2+} ions, Fig. 8.

After addition of Hg^{2+} ions added, the AgNPs show maximum peak at 430nm to SPR and the solution color selectively disappeared which observed with naked-eye, indicating of selective sensing of Hg^{2+} ions using AgNPs, Fig. 9.

The detection ability to the synthesized AgNPs was studied for various metal ions, Fig. 10. It was proved that the AgNPs were high selective to Hg^{2+} ions, with highly difference absorbance, this provide a highly indicator for qualitative and quantitative detection.

The minimum detectable Hg^{2+} ions concentration was measured using various Hg^{2+} ion concentrations with AgNPs. Fig. 11 show the photo-image of AgNPs with increasing Hg^{2+} ion concentrations, conformed the gradually loss of color with decrease in peak absorbance of SPR with a blue shift from 430 nm through addition of 0.05 ppm Hg^{2+} ions.

At first concentration of 0.05ppm, only decrease of AgNPs absorbance intensity was showed with gradually decreased and completely disappeared at 30ppm of Hg^{2+}

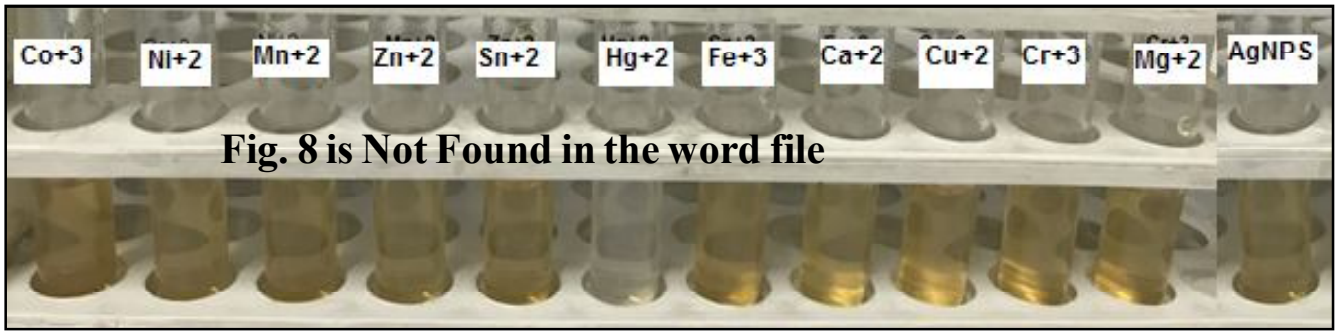

Fig. 8: Photo-image of AgNPs selectivity test following the adding of different heavy metal ions.

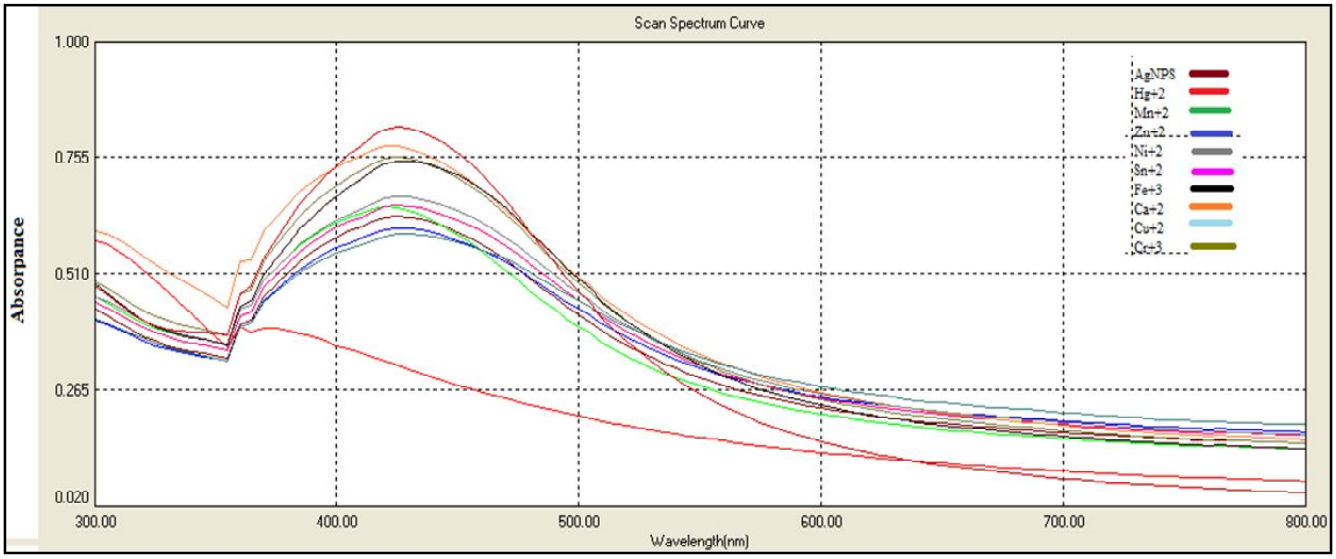

Fig. 9: UV–Vis spectra of AgNPs selectivity test after adding different heavy metal ions.

ions. Notable, upon the adding of Hg^{2+} ions, the maximum SPR of AgNPs undergo blue shift indicated the Hg-AgNPs aggregates formation, Fig. 12. This important phenomena known as Mie blue shift (Li *et al.,* 2015) which can be explained as decreasing of particle diameter as well as the NPs distance be nearer through Hg^{2+} reduction by AgNPs, so the frequencies were increased with shortening their wavelength simultaneously.

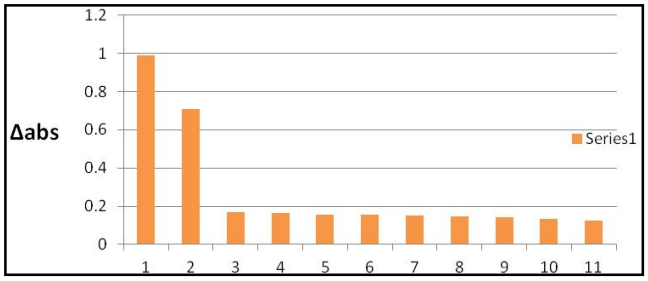

Fig. 10: The AgNPs colorimetric response in the presence of various metal ions.

The LOD of Hg^{2+} ions were determined by the distinctive SPR band of synthesized AgNPs. A linear relationship (y = 0.3497+0.0125x, linear regression coefficient, R^2 = 0.9919) was plotted among the measured absorbance at 430nm vs. Hg^{2+} ion concentration ranged from 0.05 to 30ppm, Fig. 13. The LOD was calculated as 3 times standard deviation using the formula: LOD=3Sd/s, where (SD) = standard deviation of blank solution, while (s) = Slope of the calibration graph. So, proposed mechanism for addition of Hg^{2+} ions into the AgNPs solution as selective colorimetric sensing could be an amalgamation process. Hence, this experimentation confirms that the prepared AgNPs is a suitable for quantitative determination of Hg^{2+} ions using colorimetric method in aqueous solutions, with LOD equal to 0.1 ppm.

Bio-components in Ginger extract responsible for AgNPs formation by reduction of Ag^{+} to Ag°, Also acts as a cap and stabilized agents. In addition, the Hg^{2+}

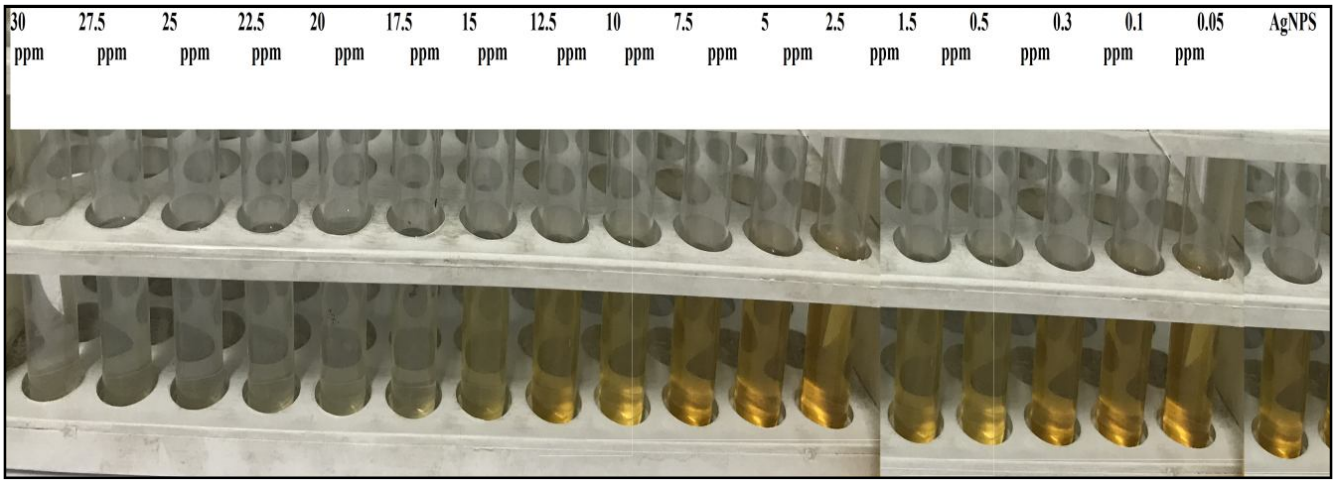

Fig. 11: Photo-image of AgNPs with increasing Hg^{+2} ion concentrations indicated the gradually loss of color.

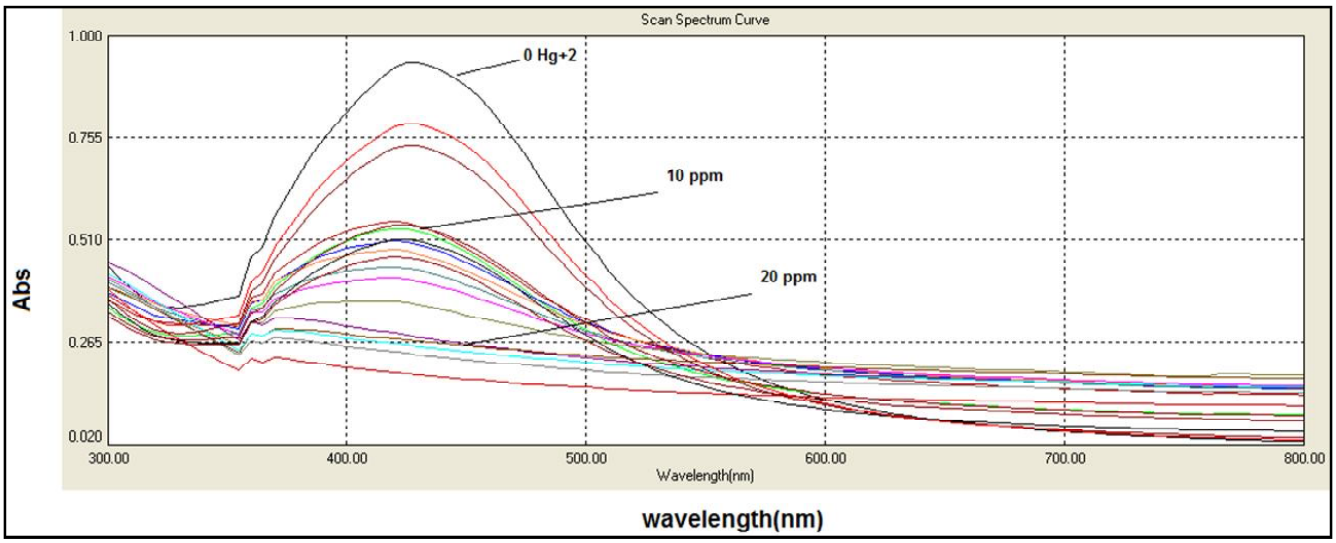

Fig. 12: Change in UV-Vis spectra of AgNP with Hg^{2+} ion concentrations increasing. A significant blue shift (decreased the peak absorbance) was shown with increasing Hg^{2+} ion concentrations.

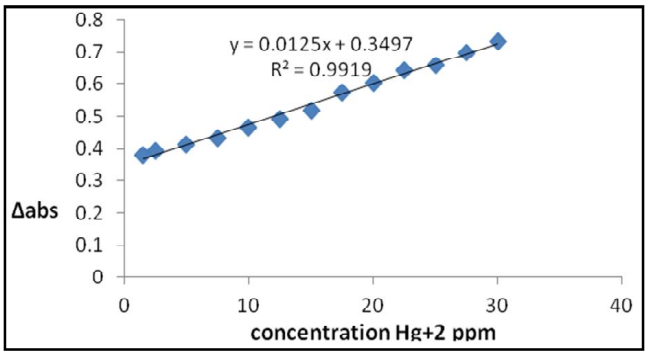

Fig. 13: Plot of absorbance measured at 430 nm vs. Hg^{2+} ion concentrations.

standard reduction potential, E° = +0.92 V has a high value than Ag^{+} standard reduction potential, E° = +0.80 V, proposing that the Hg^{2+} ion may be act as an oxidize agent. The oxidation of AgNPs occurs owing to the difference in the reduction potential changed the Hg^{2+} to Hg° and prepared Ag-Hg amalgam (Firdaus *et al.*, 2017). Therefore, change in prepared AgNPs color from yellowish-brown to colorless, as exposed in starting $AgNO_3$ colorless solution. Different mechanism could be explain in gold nanoparticles (AuNPs), Au^{3+} has a high standard reduction potential, E° = +1.40V, therefore Hg^{2+} cannot oxidize Au° of AuNPs to Au^{3+} as it take place in AgNPs (Li *et al.,* 2015).

Determination of Hg^{2+} in water and bovine serum samples

With the aim of examination the proposed method as capability of the AgNPs in life aqueous examples, these AgNPs were apply to determine the Hg^{2+} in Diyala river, tap water sample and bovine serum. Even so, we are not capable to check Hg^{2+} ions in these samples since; it's low concentration which it's lesser than the limit of detection of this process, also, we have achieved a recovery analysis method in these life aqueous samples for detection of Hg^{2+} ions. Experimentally, we have prepared two spiked constant Hg^{2+} concentrations for checking the recovery, RSD, Confidence Limited and RE% of the suggested method in: river water, tap water and bovine serum samples. The results show acceptable recovery and RSD% value of each sample, Table 2. The data indicated that the bio prepared AgNPs could be used for the Hg^{2+} determination in different real aqueous samples.

Table 2: Recovery, RSD, Confidence Limited and RE % of Hg^{2+} in life samples (n=2).

Sample	Added Hg^{+2} ppm	Found	Recovery %	RSD %	Confidence Limited	RE %
Tap water	0	ND	—	—		
	6.66	6.624 ± 0.056	99.4	0.85	7.13_6.13	0.54
	20	20.624±0.056	103	0.27	21.124_20.124	3.12
Lake water	0	ND	—	—		
	6.66	6.542± 0.059	98	0.9	7_6	1.14
	20	20.1± 0.1	100.5	0.75	21_19.2	0.5
Bovine serum	0	ND	—	—		
	6.66	6.704 ±0.056	101	0.84	7.2_6.2	0.66
	20	20.224 ±0.056	101	0.27	20.7_19.7	1.12

Conclusions

A new green-chemistry, low-cost, easy-to-use, rapidly analytical colorimetric determination of mercury by use AgNPs was enhanced. The preparation of AgNPs can be done at room temperature within 50 min and heating at 100°C. The water-soluble bio-components from Ginger extract that which acts as bio-reduction of Ag^{+} to produce steady AgNPs, which have a yellowish-brown color through SPR band at 430 nm. SEM, AFM images showed that NPs had spherical morphology. Furthermore, UV-Vis, FTIR, Zeta-potential analysis were carried out to identify the possible bio-components. The biosynthesized AgNPs show excellent efficiency to detect Hg^{2+} ions and the color changed linearly from the yellowish-brown to colorless through the increasing of Hg^{2+}ion concentration in aqueous media.

Moreover, the proposed method shows high Hg^{2+} ions selective as well as sensitive in attendance of other metals. Through using UV-Vis technique, the LOD of the suggested procedure was 0.1ppm. Therefore, the results obtained from this proved procedure have been useful and valid for the detection of Hg^{2+} ions in all real aqueous samples.

Acknowledgements

The authors thank Mustansiriyah University (www.uomustansiriyah.edu.iq), Baghdad, Iraq, for helpful to complete this work.

References

Al-Alwani, M.A. *et al.,* (2015). Effect of solvents on the extraction of natural pigments and adsorptionon to TiO2 for dye sensitized solar cell applications. Spectrochimica Acta Part A: *Molecular and Biomolecular Spectroscopy,* **138:** p.130-137.

Annadhasan, M. and N. Rajendiran (2015). Highly selective and sensitive colorimetric detection of Hg(II) ions using green synthesized silver nanoparticles, *RSC Adv.* **5:** 94513–94518.

Atkins, P. and J. de Paula (2009). Physical Chemistry, 9th ed., WH Freeman, Oxford.

Awad, M.A, A.A. Hendi, K.M.O. Ortashi, D.F.A.

Elradi, N.E. Eisa, L.A. Al-lahieb, S.M. Al-Otiby, N.M. Merghani and A.A.G. Awad (2014). Silver nanoparticles biogenic synthesized using an orange peel extract and their use as an anti-bacterial agent, *Int. J. Phys. Sci.,* **9(3):** 34-40.

Ayranci, R., D.O. Demirkol, S. Timur and M. Ak (2017). Rhodamine-based conjugated polymers: potentiometric, colorimetric and voltammetric sensing of mercury ions in aqueous medium, *Analyst,* **142:** 3407–3415.

Bernhoft, R.A. (2012). Mercury toxicity and treatment: a review of the literature. J. Environ. Public Health.

Behravan, M., A.H. Panahi, A. Naghizadeh, M. Ziaee, R. Mahdavi and A. Mirzapour (2019). Facile Green Synthesis of Silver Nanoparticles Using *Berberis vulgaris* Leaf and Root Aqueous Extract and Its Antibacterial Activity. *Int. J. Biol. Macromol.,* **124:** 148–154.

Chowdhury, I.H., S. Ghosh, M. Roy and M.K. Naskar (2015). Green synthesis of water-dispersible silver nanoparticles at room temperature using green carambola (star fruit) extract *J. Sol-Gel Sci. Technol.,* **73:** 199.

Chen, N., Y. Zhang, H. Liu, X. Wu, Y. Li, L. Miao, Z. Shen and A. Wu (2016). High-performance colorimetric detection of Hg^{2+} based on triangular silver nanoprisms, *ACS Sens,* **1:** 521–527.

Clarkson, T.W., L. Magos and G.J. Myers (2003). The toxicology of mercury–current exposures and clinical manifestations, *N. Engl. J. Med.,* **349:** 1731–1737.

Cuendet. M., *et al.,* (1997). Iridoid glycosides with free radical scavenging properties from *Fagraea blumei*. *Helvetica Chimica Acta.,* **80(4):** p. 1144-1152.

Dinda, G., D. Halder, A. Mitra, N. Pal, C. Vazquez and L.M.A. Quintela (2017). Study of the Antibacterial and Catalytic Activity of Silver Colloids Synthesized Using the Fruit of *Sapindus mukorossi*. *New J. Chem.,* **41:** 10703–10711.

Farhadia, K., M. Forougha, R. Molaeia, S. Hajizadeha and A. Rafipourb (2012). Highly selective Hg^{2+} colorimetric sensor using green synthesized and unmodified silver nanoparticles. Sensors and Actuators B: Chemical, Elsevier. P. 883.

Firdaus, M.L., S. Andriana, W. Elvinawati Alwi, E. Swistoro, A. Ruyani and A. Sundaryono (2017). Green synthesis of silver nanoparticles using *Carica papaya* fruit extract under sunlight irradiation and their colorimetric detection of mercury ions *J. Phys.: Conf. Ser.,* **817:** 012029.

Firdaus, M.L., I. Fitariani, S. Wyantuti, Y.W. Hartati, R. Khaydarov, J.A. Mcalister, H. Obata and T. Gamo (2017). Colorimetric detection of mercury (II) ion in aqueous solution using silver nanoparticles, *Anal. Sci.,* **33:** 831–837.

Hamouda, R.A., M.H. Hussein, R.A. Abo-elmagd and S.S. Bawazir (2019). Synthesis and biological characterization of silver nanoparticles derived from the cyanobacterium *Oscillatoria limnetica*. *Scientific Reports,* **9:** P.1.

Huang, D., B. Ou and R.L. Prior (2005). The chemistry behind antioxidant capacity assays. *Journal of agricultural and food chemistry,* **53(6):** p. 1841-1856.

Huang, J.T., X.X. Yang, Q.L. Zeng and J. Wang (2013). A simple green route to prepare stable silver nanoparticles with pear juice and a new selective colorimetric method for detection of cysteine. *Analyst,* **138:** 5296.

Jagtap, U.B. V.A. Bapat (2012). Green synthesis of silver nanoparticles using *Artocarpus heterophyllus* Lam. seed extract and its antibacterial activity, *Industrial Crops and Products, 46:* 132-137.

Karthiga, D. and S.P. Anthony (2013). Selective colorimetric sensing of toxic metal cations by green synthesized silver nanoparticles over a wide pH range. *RSC Adv.,* **3:** 16765.

Ke, J., X. Li, Q. Zhao, Y. Hou and J. Chen (2014). Ultra sensitive quantum dot fluorescence quenching assay for selective detection of mercury ions in drinking water, *Sci. Rep.,* **4:** 5624.

Kim, K.M., Y. Nam, Y. Lee and K. Lee (2018). A Highly Sensitive and Selective Colorimetric Hg^{2+} Ion Probe Using Gold Nanoparticles Functionalized with Polyethyleneimine. *Journal of Analytical Methods in Chemistry,* **4:** P.

Kumar, S., W. Bhattacharya, M. Singh, D. Halder and A. Mitra (2017). Plant Latex Capped Colloidal Silver Nanoparticles: A Potentanti-Biofilm and Fungicidal Formulation. *J. Mol. Liq.,* **230:** 705–713.

Kumar, S., D. Halder and A. Mitra (2017). Characterization of Silver Nanoparticles Synthesized Using Latex of *Jatropha curcas* and *Lannea grandis*. *J. Surface Sci. Technol.,* **32:** 115–120 .

Kumar, S., D. Halder and A. Mitra (2017). Centellaasiatica Leaf Mediated Synthesis of Silver Nanocolloid and Its Application as Filler in Gelatin Based Antimicrobial Nanocomposite Film. *LWT – Food Sci. Technol.,* **75:** 293–300.

Kumar, S., M. Singh, D. Halder and A. Mitra (2016). *Lippia javanica*: a Cheap Natural Source for the Synthesis of Antibacterial Silver Nanocolloid. *Appl. Nanosci.,* **6:** 1001–1007.

Kumar, V., D.K. Singh, S. Mohan, D. Bano, R.K. Gundampati and S.H. Hasan (2017). Green synthesis of silver nanoparticle for the selective and sensitive colorimetric detection of mercury (II) ion, *J. Photo. Biol. B.,* **168:** 67–77.

Keyune, B. (2017). Atomic Force Microscopy. Lappeenranta University Of Technology, Finland.

Li, J., S. Fan, Z. Qiu, C. Li and S. Nie (2015). Total flavonoids content, antioxidant and antimicrobial activities of extracts from *Mosla chinensis maxim. Cv. Jiangxiangru*. *LWT. Food Sci. Technol.,* **64:** 1022–1027.

Li, H., F. Li, C. Han, Z. Cui, G. Xie and A. Zhang (2010). Highly sensitive and selective tryptophan colorimetric sensor based on 4, 4-bipyridine-functionalized silver

nanoparticles. *Sens. Actuators, B,* **145:** 194.

Megarajan, S., K.B. Ahmed, G.K. Reddy, P.S. Kumar and V. Anbazhagan (2016). Phytoproteins in green leaves as building blocks for photosynthesis of gold nanoparticles: an efficient electrocatalyst towards the oxidation of ascorbic acid and the reduction of hydrogen peroxide. *J. Photochem. Photobiol.,* **155:**.

Mostafa, N.M. (2018). Antibacterial Activity of Ginger (*Zingiber officinale*) Leaves Essential Oil Nanoemulsion against the Cariogenic *Streptococcus mutans*, *Journal of Applied Pharmaceutical Science,* **8(09):** 034-041.

Mousavi, S.Z., S. Nafisi and H.I. Maibach (2017). Fullerene nanoparticle in dermatological and cosmetic applications. *Nanomedicine,* **13:** 1071–1087.

Mostafa, N.M. and A.N. Singab (2016). After HCV eradication with Sovaldi®, can herbs regenerate damaged liver, minimize side effects and reduce the bill? *Med Aromat Plants,* **5:** 257.

Murugan, K., B. Senthilkumar, D. Senbagam and S. Al-Sohaibani (2014). Biosynthesis of Silver Nanoparticles Using *Acacia leucophloea* Extract and Their Antibacterial Activity. *Int. J. Nanomedicine,* **9:** 2431–2438.

Nan, Y., L. Fuyan, J. Tiancai, L. Chongchong, S. Hushan, W. Lei and H. Xu (2017). Biogenic synthesis of silver nanoparticles using ginger (*Zingiber officinale*) extract and their antibacterial properties against aquatic pathogens. *Acta Oceanologica Sinica,* **36(12):** P.96.

Nurmahani, M., A. Osman, A.A. Hamid, F.M. Ghazali and M.P. Dek (2012). Antibacterial property of *Hylocereus polyrhizus* and *Hylocereus undatus* peel extracts. *International Food Research Journal,* **19(1):** 77.

Okubo, T. and M. Suda (1999). Absorption of Polyelectrolytes on Colloidal Surfaces as Studied by Electrophoretic and Dynamic Light-Scattering Techniques. *Journal of colloid and interface science,* **213(2):** 565-571.

Prasad, K.Sh., G. Shruthi and Ch. Shivamallu (2018). Functionalized Silver Nano-Sensor for Colorimetric Detection of Hg^{2+} Ions: Facile Synthesis and Docking Studies. Sensors journal. p.1.

Priyadarshini, K.A., K. Murugan, C. Panneerselvam, S. Ponarulselvam, J.S. Hwang and M. Nicoletti (2012). Biolarvicidal and Pupicidal Potential of Silver Nanoparticles Synthesized Using *Euphorbia hirta* against *Anopheles stephensi liston* (Diptera:Culicidae). *Parasitol. Res.,* **111:** 997–1006.

Rajakannu, S. *et al.,* (2015). Biosynthesis of Silver Nanoparticles using *Garcinia mangostana* Fruit Extract and their Antibacterial, Antioxidant Activity. *Int. J. Curr. Microbiol. App. Sci.,* **4:** p. 944-952.

Shimada, K. *et al.,* (1992) Antioxidative properties of xanthan on the autioxidation of soybean oil in cyclodextrin emulsion. *J. Agric Food Chem.,* **40:** 945-948.

Sivasothy, Y, W.K. Chong, A. Hamid, I.M. Eldeen, S.F. Sulaiman and K. Awang (2011). Essential oils of *Zingiber officinale var. rubrum* Theilade and their antibacterial activities. *Food Chem.,* **124:** 514-517.

Samrot, A.V., N. Shobana and R. Jenna (2018). Antibacterial and Antioxidant Activity of Different Staged Ripened Fruit of *Capsicum annuum* and Its Green Synthesized Silver Nanoparticles. *Bionano. sci.,* **8:** 632–646.

Samrot, A.V., P. Raji, A.J. Selvarani and P. Nishanthini (2018). Antibacterial Activity of Some Edible Fruits and Its Green Synthesized Silver Nanoparticles against Uropathogen–*Pseudomonas aeruginosa* SU 18. *Biocatal. Agric. Biotechnol.,* **16:** 253–270.

Surya, G.S., D. Kumar and R. Rajakumar (2016). Green Synthesis of Silver Nanoparticles from Flower Extract of *Hibiscus rosa-sinensis* and Its Antibacterial Activity. *International Journal of Innovative Research in Science Engineering and Technology,* **5(4):** P.3.

Wang, Y., F. Yang and X. Yang (2010). Colorimetric detection of mercury (II) ion using unmodified silver nanoparticles and mercury- specific oligonucleotides, *Appl. Mat. Interfaces,* **2:** 339–342.

Xu, D., S. Yu, Y. Yin, S. Wang, Q. Lin and Z. Yuan (2018). Sensitive Colorimetric Hg^{2+} Detection via Amalgamation-Mediated Shape Transition of Gold Nanostars. *Frontiers in Chemistry,* **6:** p.3.

Yang, Z., W. Yang, Q. Peng, Q. He, Y. Feng, S. Luo and Z. Yu (2009). Volatile phytochemical composition of rhizome of ginger after extraction by headspace solid-phase micro extraction, petroleum ether extraction and steam distillation extraction. *Bangladesh J. Pharmacol.,* **4:** 136-143.

Yuan, M., Y. Li, J. Li, C. Li, X. Liu, J. Lv, J. Xu, H. Liu, S. Wang and D. Zhu (2007). A colorimetric and fluorometric dual-modal assay for mercury ion by a molecule, *Org. Lett.,* **9(23):** 13–2316.

Yoosaf, K., B.I. Ipe, C.H. Suresh and K.G. Thomas (2007) In situ synthesis of metal nanoparticles and selective naked-eye detection of lead ions from aqueous media. *J. Phys. Chem.,* **111:** 12839.

Zhang, D., B. Gökce and S. Barcikowski (2017). Laser synthesis and processing of colloids: fundamentals and applications, *Chem. Rev.,* **117:** 3990-4103.